TECHNICAL MEMORANDUM

ANL-CT-77-4

A MATHEMATICAL MODEL FOR CROSS-FLOW-INDUCED VIBRATIONS OF TUBE ROWS

by

S. S. Chen

Components Technology Division
Argonne National Laboratory
Argonne, Illinois

Base Technology

September 1976

DISCLAIMER

The facilities of Argonne National Laboratory are owned by the United States Government. Under the terms of a contract (W-31-109-Eng-38) between the U. S. Energy Research and Development Administration, Argonne Universities Association and The University of Chicago, the University employs the staff and operates the Laboratory in accordance with policies and programs formulated, approved and reviewed by the Association.

MEMBERS OF ARGONNE UNIVERSITIES ASSOCIATION

The University of Arizona
Carnegie-Mellon University
Case Western Reserve University
The University of Chicago
University of Cincinnati
Illinois Institute of Technology
University of Illinois
Indiana University
Iowa State University
The University of Iowa
Kansas State University
The University of Kansas
Loyola University
Marquette University
Michigan State University
The University of Michigan
University of Minnesota
University of Missouri
Northwestern University
University of Notre Dame
The Ohio State University
Ohio University
The Pennsylvania State University
Purdue University
Saint Louis University
Southern Illinois University
The University of Texas at Austin
Washington University
Wayne State University
The University of Wisconsin

TECHNICAL MEMORANDUM

ANL-CT-77-4

LMFBR Components
(UC-79k)

A MATHEMATICAL MODEL FOR CROSS-FLOW-INDUCED VIBRATIONS OF TUBE ROWS

by

S. S. Chen

U of C-AUA-USERDA

Components Technology Division
Argonne National Laboratory
Argonne, Illinois

Base Technology

September 1976

ABSTRACT

Flow-induced vibrations in heat exchanger tube banks are well known. Tube vibrations have resulted in failure due to mechanical wear, fretting corrosion, and fatigue cracking. The detrimental effect of flow-induced vibrations has led to numerous investigations for a better understanding of the phenomena in heat exchangers, particularly in high temperature, high performance heat exchangers used in nuclear reactor systems.

Several excitation mechanisms have been considered including vortex shedding, fluidelastic excitation, jet switching, turbulence buffeting, and acoustic excitation. Based on different excitation mechanisms, different mathematical models have been developed. As we know, a tube bank may be subjected to several excitations simultaneously, and sometimes it is difficult to identify which is the dominant excitation. A model considering only a single excitation mechanism is obviously inadequate. Furthermore, those models do not account for all the fluid coupling in a tube bank. Therefore, the objective of this report is to propose a mathematical model including multiple tubes and multiple excitation mechanisms.

The mathematical model presented in this report includes the effects of vortex shedding, fluidelastic coupling, drag force, and fluid inertia coupling. Once the fluid forces are known, the model can predict the details of complex tube-fluid interactions: (1) natural frequencies and mode shapes of coupled vibrations; (2) critical flow velocities; (3) responses to vortex shedding, drag force, and other types of excitations; and (4) the dominant excitation mechanism at a given flow velocity. The analytical results are in good agreement with the published experimental results. The following are some general conclusions: (a) Multiple tubes must be considered in a mathematical model for closely spaced tube banks in a dense fluid. (b) Tube banks respond as an integrated system rather than

as a collection of many individual tubes. (c) Natural frequencies of tube banks increase slightly with increasing crossflow velocity. (d) Flutter flow velocity may be smaller or larger than that associated with vortex shedding. (e) Detuning the tubes has a beneficial effect on stability. (f) Flutter flow velocity varies with tube number and system damping. (g) The most critical instability mode is associated with the motion involving a tube vibrating predominantly in the streamwise direction, while its two neighboring tubes vibrate predominantly in the transverse direction with a phase shift of 180°. (h) Fluidelastic coupling makes tube motion orbital.

In conclusion, there is a great need for a useful mathematical model for cross-flow-induced vibrations of tube banks. The model presented in this report has demonstrated that it is capable of predicting the details of tube-fluid interactions including instabilities and responses to various types of excitations. With this model, improved design criteria can be established to eliminate detrimental flow-induced vibrations in tube banks.

TABLE OF CONTENTS

LIST OF ILLUSTRATIONS

LIST OF TABLES

NOMENCLATURE

a_{im}, b_{im}	Generalized coordinates
c_i	Viscous damping coefficient associated with the motion in the x direction
c^{ℓ}, c_i^{ℓ}	Lift coefficients
c_i^d	Drag coefficient
d	Tube diameter
e_i	Viscous damping coefficient associated with the motion in the y direction
e_o	Reference viscous damping coefficient
E_i	Young's modulus
f_c	Natural frequency of coupled mode
f_i, g_i	Total external forces per unit length
f_i^c, g_i^c	Fluid inertia forces
f_i^h, g_i^h	Hydrodynamic damping
f^{ℓ}, f_i^{ℓ}	Lift forces
f_i^e, g_i^e	Fluidelastic forces
f_i^o, g_i^o	External forces associated with other flow noises
f_{im}, g_{im}	Generalized forces given in Eq. (17)
g_i^d	Drag force
G	Gap
I_i, J_i	Moment of inertia in the x and y directions
k	Number of tubes
ℓ	Tube length
L	Mass matrix given in Eq. (19)
m_i	Tube mass per unit length
M'	Displaced mass of fluid per unit length
q_m	Generalized forces given in Eq. (17)
Q	Generalized force vector

NOMENCLATURE (Contd.)

R	Damping matrix given in Eq. (19)
S	Strouhal number
t	Time
T	Stiffness matrix given in Eq. (19)
u_i	Tube displacement in the x direction
v_i	Tube displacement in the y direction
V	Flow velocity
V_{cr}	Critical flow velocity
x,y,z	Cartesian coordinates
α_{ij},β_{ij}	Added mass coefficients
σ_n	Eigenvalue of added mass matrix
ϵ_i	A small number
ζ_c	Modal damping ratio of coupled mode
ζ_{im},η_{im}	Modal damping ratios given in Eq. (17)
λ	Eigenvalue of Eqs. (23) and (24)
$\mu_i,\mu_i',\mu,$ μ_{ij},μ_{ij}'	Fluidelastic coefficients
$\nu_i,\nu_i',\nu,$ ν_{ij},ν_{ij}'	Fluidelastic coefficients
ρ	Fluid density
$\sigma_{ij},\sigma_{ij}',$ τ_{ij},τ_{ij}'	Hydrodynamic damping coefficients
$\phi_i(z)$	Orthonormal function of tube in vacuo
ψ_i^{ℓ},ψ_i^{d}	Phase angles of lift and drag forces
$\omega_{im},\bar{\omega}_{im}$	Natural frequencies of tubes in vacuo
ω_s	Circular frequency of vortex shedding
Ω	Circular frequency
Ω_n	Natural frequency of coupled modes

I. INTRODUCTION

Flow-induced vibrations in heat exchanger tube banks are well known. Tube vibrations have resulted in failure due to mechanical wear, fretting corrosion, and fatigue cracking [1]. The detrimental effect of flow-induced vibrations has led to numerous investigations for a better understanding of the phenomena in heat exchangers, particularly in high temperature, high performance heat exchangers used in nuclear reactor systems.

From a practical point of view, what heat exchanger designers need is to know when and why flow-induced vibration or instability occurs and how to suppress them. To be able to answer these questions, one must understand the mechanisms involved. Several excitation mechanisms are briefly reviewed as follows:

A. Vortex Shedding

Vortex induced vibration of tube banks has been extensively studied by Chen [2,3] and others. When one of the natural frequencies of a tube bank is near the Strouhal frequency, the tubes can be excited to have large oscillations. Although vortex shedding process will be modified by tube motions and synchronizes with tube oscillations, it is the vortex shedding that initiates tube vibration.

Vortex shedding can induce transverse tube oscillations. In dense fluid, drag force can also induce tube oscillations in the streamwise direction. Coupled vibration of multiple tubes in the flow direction has been observed by King and Johns [4]. In light fluid, if tubes are given a relatively large motion in the flow direction, tube oscillations in the flow direction are also possible. This has been demonstrated by Griffin and Ramberg for a single tube in wind tunnel [5].

Based on the vortex shedding theory, if one knows the Strouhal number as a function of the array geometry, the flow velocity at which resonance

occurs can be predicted. However, there is little detailed information on the velocity range over which "lock-in" occurs, orbital paths of tube motions, and amplitudes of tube displacements. One of the main assumptions in this theory is the existence of vortex shedding within tube banks. Although many investigators have measured the Strouhal number in tube banks, summarized recently by Fitz-Hugh [6], it is still questionable whether vortex shedding exists in the middle of tube banks.

B. Fluidelastic Instability

Connors is the first investigator recognizing the fluidelastic mechanism of tube banks subject to cross flow [7]. The instability belongs to the classical flutter phenomenon which has been extensively studied in aerospace industry. The essential parameters associated with this mechanism are system damping and fluidelastic forces. When the flow velocity is increased to a certain value, the work done on the tube system by fluidelastic forces will be larger than dissipation by damping; therefore, large-amplitude oscillations will occur. Based on the experimentally observed tube oscillations and measured fluidelastic coefficients, Connors developed a simple instability criterion for crossflow-induced instability of tube-rows by analyzing the motion of a single tube in a tube row.

Fluidelastic instability has been further considered by Blevins [8], Gorman and Mirza [9], Halle et al. [10], and Erskine and Waddington [11]. However, the dependence of fluidelastic-instability thresholds for tube banks on system parameters, such as tube pattern, tube pitch, individual tube natural frequencies, and tube damping, is not well understood. The mathematical approach used by Blevins [8] includes multiple tubes with fluidelastic coupling but fluid inertia coupling, which is important for tube banks vibrating in dense fluid, is not accounted. Furthermore, in

existing mathematical models, the tubes are assumed to be in tune; variations in tube properties have not been considered.

C. Turbulent Excitations

In a tube bank, there exist random flow noises including turbulent pressure fluctuations and far-field flow noises with some or little coherence. When tubes are subjected to those random excitations, the tubes will respond primarily at the natural frequencies of the system. Owen [12] has made one of the most complete theoretical approaches to this problem. He disregards any theory of a superposed regular pattern of excitations.

If one knows turbulence spectrum and spatial correlation in a tube bank and assumes that structural oscillations do not affect the fluid pressure field, it is possible to calculate tube-bank responses. However, very little has been done in literature for tube banks.

In a flow loop, turbulent pressure fluctuations and other flow noises will always exist; the magnitudes of those noises are, most likely, system dependent. In modeling a tube bank, the random flow noises should be accounted for in addition to other excitations.

D. Acoustic Excitations

Acoustic excitations can cause tube vibration normal to the flow direction and tube axis. When the natural frequency of vortex shedding at a particular flow rate coincides with the acoustic frequencies, two systems (fluid flow and acoustic field) are coupled and reinforce each other. The worst case is that when acoustic frequency, tube frequency and vortex-shedding frequency are the same [13,14,15].

Little consideration has been given to the interactions of acoustic waves with tube banks in the past. The problem includes transmission, scattering, and radiation of acoustic waves by a group of elastic tubes. Obviously it is not an easy problem to solve, particularly when acoustoelastic

vibration is coupled to vortex shedding process. Nevertheless, when acoustic excitations are important in certain cases, its effect must be included.

Several other excitation mechanisms also have been considered; those include, among others, jet switching, structural borne noises, and flow pulsations. In some cases, those excitations may be important. However, it is believed that, in most cases, the four mechanisms reviewed are the most important ones.

Based on the brief review, we observed that: (1) a single excitation mechanism, either self-excited or forced vibration, is considered in the past; and (2) in most cases, a single tube is taken as a model for tube banks without including all the fluid coupling effects. In reality, a tube bank may be subjected to several types of excitations simultaneously and sometimes it is difficult to identify which is the dominant excitation; considering only one excitation mechanism is not sufficient. Furthermore, a tube bank will vibrate as a group rather than as an isolated tube. Without including all the fluid coupling effects, the vibrational modes of tube banks cannot be described. Therefore, it is clear that a mathematical model including multiple excitation mechanisms and multiple tubes is definitely needed. The objective of this report is intended to satisfy this need: presenting a mathematical model to account for multiple excitation mechanisms in tube banks using coupled modes.

II. EQUATIONS OF MOTION

A row of k tubes subjected to a cross flow is shown in Fig. 1. The axes of the tubes are parallel to the z axis and the centers of the tubes are on the x axis. Tube diameter is d and the gap between two neighboring tubes is G. The subscript i is used to denote variables associated with tube i. The variables associated with tube motion in the x direction are flexural rigidity E_iI_i, tube mass per unit length m_i, viscous damping coefficient c_i, and displacement u_i. The equation of motion for tube i in the x direction is

$$E_iI_i \frac{\partial^4 u_i}{\partial z^4} + c_i \frac{\partial u_i}{\partial t} + m_i \frac{\partial^2 u_i}{\partial t^2} = f_i \ , \ i = 1,2,3....k, \tag{1}$$

where f_i is the force per unit length acting on the tube including hydrodynamic forces and other excitations. Similarly, the equation of motion in the y direction is

$$E_iJ_i \frac{\partial^4 v_i}{\partial z^4} + e_i \frac{\partial v_i}{\partial t} + m_i \frac{\partial^2 v_i}{\partial t^2} = g_i \ , \ i = 1,2,3....k, \tag{2}$$

where E_iJ_i,* e_i, v_i and g_i are flexural rigidity, damping coefficient, displacement, and external force per unit length in the y direction.

The external forces acting on a structural element include inertia force, drag force, lift force, fluidelastic force, hydrodynamic damping and other noises; these are given by

and

$$\begin{aligned} f_i &= f_i^c + f_i^\ell + f_i^e + f_i^h + f_i^o \ , \\ g_i &= g_i^c + g_i^d + g_i^e + g_i^h + g_i^o \ . \end{aligned} \tag{3}$$

One of the major problems to calculate the response of a tube bank to a cross flow is to determine these force components.

The inertia force associated with the tube motion in fluid was studied previously [16]. f_i^c and g_i^c are as follows:

*For generality, the moments of inertia in the two directions are assumed to be different. For tubes, I_i is usually equal to J_i.

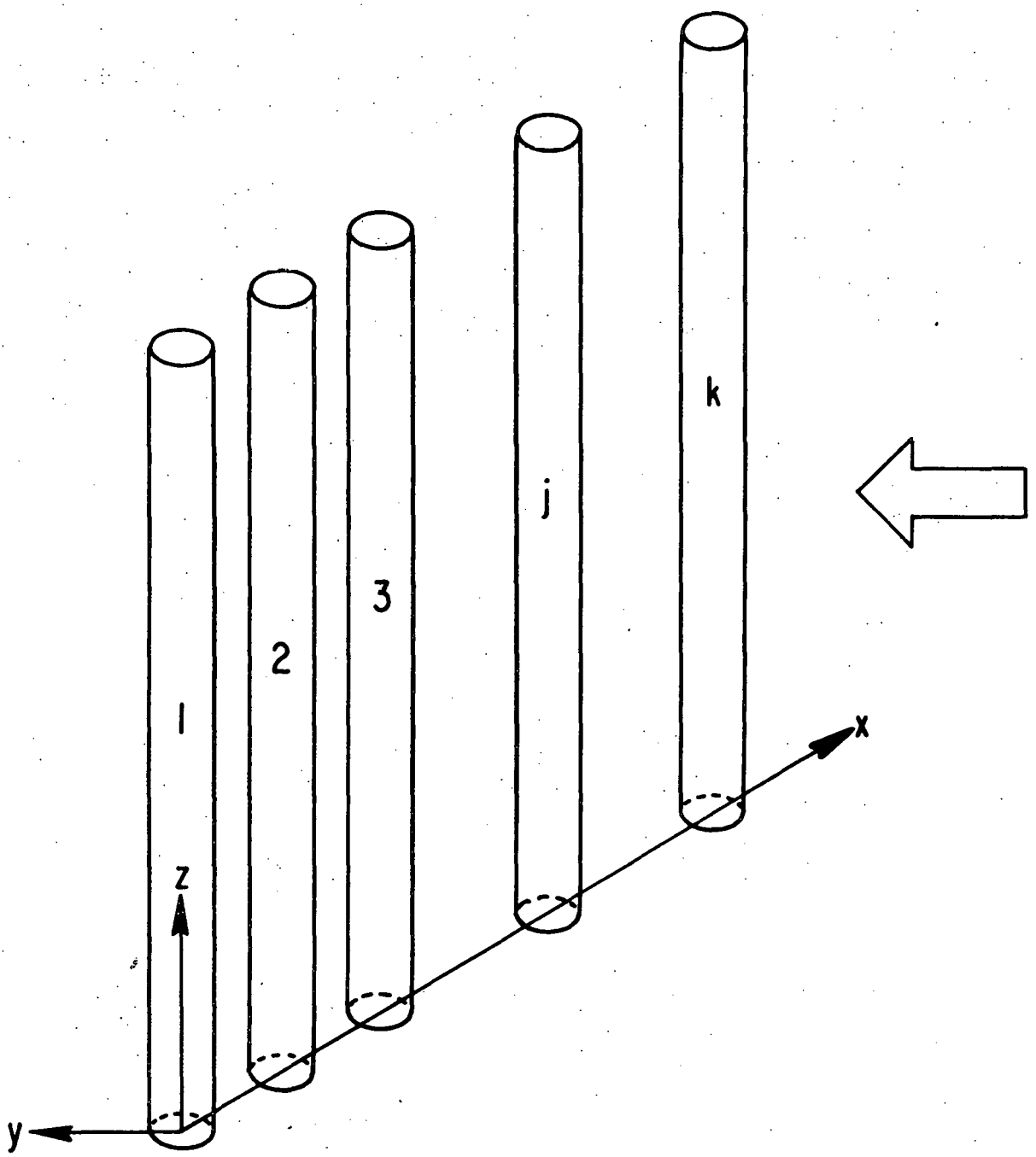

Fig. 1. Schematic of a row of tubes subjected to a cross-flow

$$f_i^c = - M' \sum_{j=1}^{k} \alpha_{ij} \frac{\partial^2 u_i}{\partial t^2} ,$$

and (4)

$$g_i^c = - M' \sum_{j=1}^{k} \beta_{ij} \frac{\partial^2 v_i}{\partial t^2} ,$$

where M' is the displaced mass of fluid by the tube, and α_{ij} and β_{ij} are added mass coefficients.

It is well known that the lift force acting on a single tube is

$$f^{\ell} = \frac{1}{2} \rho V^2 \, dc^{\ell} \sin \omega_s t, \tag{5}$$

where ρ is fluid density, V is flow velocity, c^{ℓ} is lift coefficient, and ω_s is the vortex shedding frequency given by

$$\omega_s = \frac{2\pi SV}{d} . \tag{6}$$

The Strouhal number S is equal to 0.2 for a single tube in the subcritical Reynolds number. In the case of multiple tubes, experimental results have shown that there are multiple values of S for gap-to-diameter ratio less than one. The Strouhal number obtained by various investigators [2,7,17, 18,19] for a row of tubes is shown in Fig. 2. Further investigation is required to determine the values of S, lift coefficient c^{ℓ}, and phase relation among the tubes. Without such detailed information, the lift force acting on the i tube is assumed to be

$$f_i^{\ell} = \frac{1}{2} \rho V^2 \, dc_i^{\ell} \sin (\omega_s t + \psi_i^{\ell}) , \tag{7}$$

where c_i^{ℓ} is the lift coefficient of the i tube and ψ_i^{ℓ} describes the phase relation.

The drag force consists of two parts, skin friction drag and pressure drag. For a steady flow, drag force depends on the Reynolds number and the relative roughness of the boundary surface. The results for a large number of single body appear in a number of references (e.g., Ref. 20). Unfortunately, such is not the case for a system consisting of multiple structural elements.

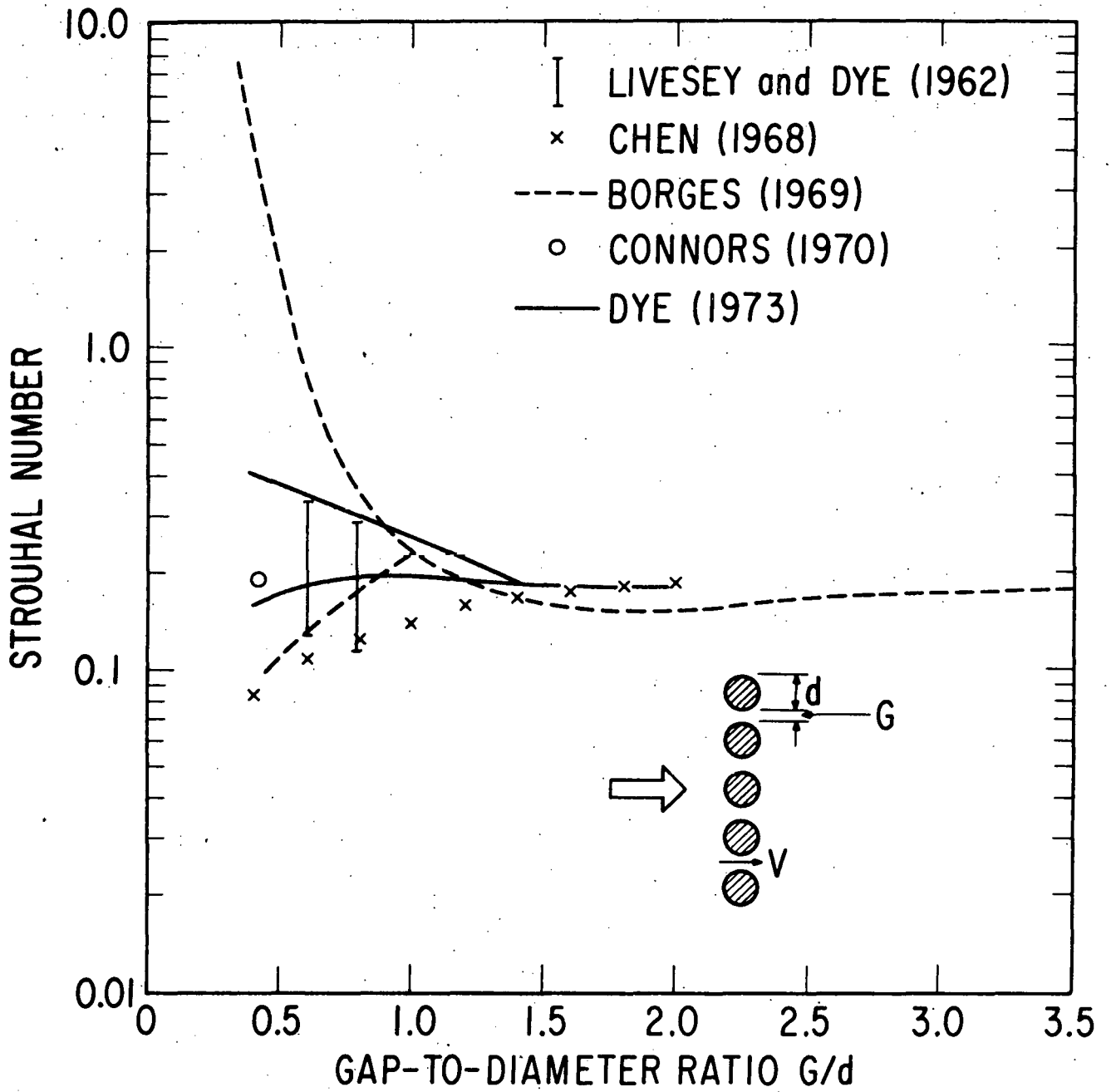

Fig. 2. Strouhal number as a function of the gap-to-diameter ratio based on gap velocity

The drag force is steady until vortex instability begins. Then it oscillates either periodically or randomly about a mean value. The drag force acting on the tube is assumed to be

$$g_i^d = \frac{1}{2} \rho V^2 \, \overline{dc_i^d} \, [1 + \epsilon_i \sin (2\omega_s t + \psi_i^d)] \, , \tag{8}$$

where c_i^d is drag coefficient of the i tube, ϵ_i is a small number, and ψ_i^d is a phase angle.

The quasi-steady fluid forces associated with tube displacements were investigated by Connors [7]. Due to the motion of the tubes, a momentary displacement of a tube in a tube bank from its equilibrium position alters the fluid field. As a result, additional fluid forces are induced. These forces may be represented by [21]

$$f_i^e = \frac{1}{2} \rho V^2 \left(\sum_{j=1}^{k} \mu_{ij} u_j + \sum_{j=1}^{k} \nu_{ij} v_j \right) \, ,$$

and (9)

$$g_i^e = \frac{1}{2} \rho V^2 \left(\sum_{j=1}^{k} \nu'_{ij} u_j + \sum_{j=1}^{k} \mu'_{ij} v_j \right) \, ,$$

where μ_{ij}, μ'_{ij}, ν_{ij}, and ν'_{ij} are fluidelastic force coefficients. For example, the fluidelastic force acting on the tube i in the x direction due to a unit displacement of tube j in the y direction is equal to $\frac{1}{2} \rho V^2 \nu_{ij}$. Theoretically, the displacement of a tube will induce a force on every tube. However, for practical purposes, the forces acting on those tubes which are far away from the moving tube are negligible. Assuming the fluidelastic forces depend only on the displacements of itself and its two neighboring tubes and using an argument of symmetry, one will obtain the following expressions for the fluidelastic forces:

$$f_i^e = \frac{1}{2} \rho V^2 \, [\mu \, (-u_{i+1} - u_{i-1} + 2u_i) + \nu \, (v_{i+1} - v_{i-1})] \, ,$$

and (10)

$$g_i^e = \frac{1}{2} \rho V^2 \, [\mu' (-v_{i+1} - v_{i-1} + 2v_i) + \nu' \, (u_{i+1} - u_{i-1})] \, .$$

Equations (10) were employed by Blevins [8] to study the stability of tube rows.

In a stationary fluid, fluid damping can be accounted for using viscous damping terms as given in Eqs. (1) and (2). Once the fluid is flowing, fluid flows will produce additional hydrodynamic damping. Based on the potential flow theory, the hydrodynamic damping associated with a tube bank subject to cross flows is given as follows [21]:

$$f_i^h = -\rho d V \left(\sum_{j=1}^{k} \sigma_{ij} \dot{u}_j + \sum_{j=1}^{k} \tau_{ij} \dot{v}_j \right) ,$$

and (11)

$$g_i^h = -\rho d V \left(\sum_{j=1}^{k} \sigma'_{ij} \dot{u}_j + \sum_{j=1}^{k} \tau'_{ij} \dot{v}_j \right) ,$$

where the dot denotes differentiation with respect to time.

Using Eqs. (1) to (11) gives

$$\begin{aligned} & E_i I_i \frac{\partial^4 u_i}{\partial z^4} + c_i \frac{\partial u_i}{\partial t} + m_i \frac{\partial^2 u_i}{\partial t^2} + M' \sum_{j=1}^{k} \alpha_{ij} \ddot{u}_j \\ & - \frac{1}{2} \rho V^2 \left(\sum_{j=1}^{k} \mu_{ij} u_j + \sum_{j=1}^{k} \nu_{ij} v_j \right) \\ & + \rho d V \left(\sum_{j=1}^{k} \sigma_{ij} \dot{u}_j + \sum_{j=1}^{k} \tau_{ij} \dot{v}_j \right) \\ & = \frac{1}{2} \rho V^2 d c_i^{\ell} \sin(\omega_s t + \psi_i^{\ell}) + f_i^o , \\ & E_i J_i \frac{\partial^4 v_i}{\partial z^4} + e_i \frac{\partial v_i}{\partial t} + m_i \frac{\partial^2 v_i}{\partial t^2} + M' \sum_{j=1}^{k} \beta_{ij} \ddot{v}_j \\ & - \frac{1}{2} \rho V^2 \left(\sum_{j=1}^{k} \nu'_{ij} u_j + \sum_{j=1}^{k} \mu'_{ij} v_j \right) \\ & + \rho d V \left(\sum_{j=1}^{k} \sigma'_{ij} \dot{u}_j + \sum_{j=1}^{k} \tau'_{ij} \dot{v}_j \right) \\ & = \frac{1}{2} \rho V^2 d c_i^{d} [1 + \varepsilon_i \sin(2\omega_s t + \psi_i^{d})] + g_i^o , \end{aligned} \qquad (12)$$

$i = 1,2,3,\ldots k.$

Equations (12) are the general equations of motion for a tube-row subject to a cross flow. Vibrations and stability of a tube row can be analyzed using these equations. Equations (12) can also be applied to tube banks if additional inertia coupling terms are included [22].

III. ANALYSIS

It is assumed that all tubes are of the same length and have the same type of boundary conditions in the x and y directions. In this case, the modal functions for tubes vibrating in the x and y directions will be the same; thus, let

$$u_i(z,t) = \sum_{m=1}^{\infty} a_{im}(t)\, \phi_m(z) \quad ,$$

and

$$v_i(z,t) = \sum_{m=1}^{\infty} b_{im}(t)\, \phi_m(z) \quad , \tag{13}$$

where $\phi_m(z)$ is the m-th orthonormal function of the tubes in vacuo; i.e.,

$$\frac{1}{\ell} \int_0^{\ell} \phi_m \phi_n dz = \delta_{mn} \quad , \tag{14}$$

where ℓ is the length of the tubes. Using Eqs. (12), (13), and (14) yields

$$m_i \omega_{im}^2 a_{im} + 2m_i \zeta_{im} \omega_{im} \dot{a}_{im} + m_i \ddot{a}_{im} + M' \sum_{j=1}^{\infty} \alpha_{ij} \ddot{a}_{jm}$$

$$- \frac{1}{2} \rho V^2 \left(\sum_{j=1}^{k} \mu_{ij} a_{jm} + \sum_{j=1}^{k} \nu_{ij} b_{jm} \right)$$

$$+ \rho d V \left(\sum_{j=1}^{k} \sigma_{ij} \dot{a}_{jm} + \sum_{j=1}^{k} \tau_{ij} \dot{b}_{jm} \right)$$

$$= q_m c_i^{\ell} \sin (\omega_s t + \psi_i^{\ell}) + f_{im} \quad , \tag{15}$$

$$m_i \bar{\omega}_{im}^2 b_{im} + 2m_i \eta_{im} \bar{\omega}_{im} \dot{b}_{im} + m_i \ddot{b}_{im} + M' \sum_{j=1}^{\infty} \beta_{ij} \ddot{b}_{jm}$$

$$- \frac{1}{2} \rho V^2 \left(\sum_{j=1}^{k} \nu'_{ij} a_{jm} + \sum_{j=1}^{k} \mu'_{ij} b_{jm} \right)$$

$$+ \rho d V \left(\sum_{j=1}^{k} \sigma'_{ij} \dot{a}_{jm} + \sum_{j=1}^{k} \tau'_{ij} \dot{b}_{jm} \right)$$

$$= q_m c_i^{d} [1 + \varepsilon_i \sin (2\omega_s t + \psi_i^{d})] + g_{im} \quad , \tag{16}$$

where ω_{im} and $\bar{\omega}_{im}$ are the m-th frequencies in vacuo for tube i in the x and y direction respectively (if $I_i = J_i$, ω_{im} will be equal to $\bar{\omega}_{im}$), and

$$
\begin{aligned}
q_m &= \frac{1}{2\ell}\rho V^2 d \int_o^\ell \phi_m(z)dz \ , \\
f_{im} &= \frac{1}{\ell}\int_o^\ell f_i^o \, \phi_m(z)dz \ , \\
g_{im} &= \frac{1}{\ell}\int_o^\ell g_i^o \, \phi_m(z)dz \ , \\
\zeta_{im} &= \frac{c_i}{2m_i\omega_{im}} \ , \\
\eta_{im} &= \frac{e_i}{2m_i\bar{\omega}_{im}}
\end{aligned}
\qquad (17)
$$

Note that equations (15) and (16) can be applied to all values of m. For each m, there are 2k equations which are coupled. However, there is no coupling among the equations for different m. This is true for a row of tubes having the same length and same type of boundary conditions. If the tubes have different types of end conditions, a similar method of analysis can be developed.

Equations (15) and (16) can be written in matrix form:

$$
\begin{aligned}
[M]\{\ddot{A}\} + [D]\{\dot{A}\} + [K]\{A\} + [H]\{\dot{B}\} + [C]\{B\} &= \{P\} \ , \\
[\bar{M}]\{\ddot{B}\} + [\bar{D}]\{\dot{B}\} + [\bar{K}]\{B\} + [\bar{H}]\{\dot{A}\} + [\bar{C}]\{A\} &= \{\bar{P}\} \ .
\end{aligned}
\qquad (18)
$$

Equations (18) may be written as a single equation

$$[L]\{\ddot{W}\} + [R]\{\dot{W}\} + [T]\{W\} = \{Q\},$$

where

$$
[L] = \begin{bmatrix} M & O \\ O & \bar{M} \end{bmatrix} \ , \ [R] = \begin{bmatrix} D & H \\ \bar{H} & \bar{D} \end{bmatrix} \ , \qquad (19)
$$

$$
[T] = \begin{bmatrix} K & C \\ \bar{C} & \bar{K} \end{bmatrix} \ , \ \{W\} = \begin{Bmatrix} A \\ B \end{Bmatrix}, \ \{Q\} = \begin{Bmatrix} P \\ \bar{P} \end{Bmatrix} \ .
$$

[L], [R], and [T] are the mass, damping, and stiffness matrices respectively and {W} and {Q} are the corresponding displacement and force vectors. When the fluid is flowing, [R] and [T] are not symmetric. Equation (19) is further reduced to

$$[U]\{\dot{\Psi}\} + [V]\{\Psi\} = \{\Gamma\} \quad , \tag{20}$$

where

$$[U] = \begin{bmatrix} 0 & L \\ L & R \end{bmatrix}, \quad [V] = \begin{bmatrix} -L & 0 \\ 0 & T \end{bmatrix},$$
$$\{\Psi\} = \begin{Bmatrix} \dot{W} \\ W \end{Bmatrix}, \quad \{\Gamma\} = \begin{Bmatrix} 0 \\ Q \end{Bmatrix} . \tag{21}$$

Equations (20) are the basic equations which are to be used in the studies of free vibration, stability, and forced vibration.

The damped free vibration mode shapes and mode values are obtained by applying solutions

$$\{\Psi\} = \{\bar{X}\} \exp(\lambda t) \tag{22}$$

to the homogeneous form of Eq. (20):

$$[\lambda U + V]\{\bar{X}\} = \{0\} \quad . \tag{23}$$

The adjoint form to Eq. (23) is

$$[\lambda U' + V']\{\bar{Y}\} = \{0\} \tag{24}$$

where ' denotes the transport of a matrix. The solutions of Eqs. (23) and (24) can be achieved by standard procedures. Assuming that the modal matrices obtained from Eqs. (23) and (24) are [X] and [Y] respectively. Let

$$\{\Psi\} = [X]\{\Phi\} \quad . \tag{25}$$

Substituting Eq. (25) into (20) and using the biothorgonability condition yields

$$[E]\,\dot{\Phi} + [F]\,\Phi = [Y']\{\Gamma\} \quad , \tag{26}$$

where E and F are diagonal and hence Eq. (26) are uncoupled and easily solved.

IV. RESULTS

For presentation, stainless steel tubes with the following properties are considered: outside diameter 2.223 cm (0.875 in.), wall thickness 0.114 cm (0.045 in.), and length 101.6 cm (40 in.). The gap G is 0.911 cm (0.359 in.). All tubes are assumed to be simply-supported at both ends, and containing sodium and submerged in a sodium flow at 516°C (960°F). In this case, the natural frequency for a single tube in sodium is 36.01 Hz in both directions. The viscous damping coefficient c_i and e_i is assumed to be 6.895 Pa-sec (0.001 lb-sec/in.^{2}) for all tubes.

Once tube arrangement is known, added mass coefficients, α_{ij} and β_{ij}, can be calculated [16,22]. As long as the tube motion is small, the potential flow theory will give sufficiently accurate results. Since, in most cases, we are interested in small-amplitude oscillations or incipient-instability motion, the potential flow theory is applicable.

Fluidelastic coefficients can be obtained as follows: First, measure the steady fluid forces acting on each tube in the x and y directions; those force components are designated by f_i' and g_i' respectively. Then displace tube j in the x direction with a small displacement u_j, measure the steady force components again; those are designated by f_i'' and g_i''. Fluidelastic coefficients μ_{ij} and ν_{ij} can be calculated from these force components:

$$\mu_{ij} = \frac{f_i'' - f_i'}{\frac{1}{2}\rho V^2 u_j} \quad ,$$

and (27)

$$\nu'_{ij} = \frac{g_i'' - g_i'}{\frac{1}{2}\rho V^2 u_j} \quad .$$

Similarly, μ'_{ij} and ν_{ij} can be calculated by displacing tube j in the y direction.

Hydrodynamic damping can also be obtained experimentally. Unlike fluidelastic coefficients, the experimental determination of hydrodynamic damping

coefficients will require a dynamic method of analysis and involve a great amount of measurement.

To the author's knowledge, there is no other experimental data available except those measured by Connors [7] on fluidelastic forces. It is recognized that Connors obtained fluidelastic coefficients from an energy consideration for an idealized mode shape and with relatively large displacements. His results may not be the same as those calculated from Eqs. (27). However, without other detailed information on fluidelastic coefficients and Connors' data representing the best information available to date, his data will be used in the following calculations. Therefore, fluidelastic forces are based on Eq. (10). Connors did not give the data for μ and μ' and they will be assumed to be zero (in reality, μ and μ' are not zero). The values of ν and ν' are 0.101 and 0.165 respectively. Since there is no experimental data for hydrodynamic damping, it will not be included in the following calculations (i.e., σ_{ij}, τ_{ij}, σ'_{ij}, $\tau'_{ij} = 0$).

In view of the fact that there is insufficient information on fluidelastic and hydrodynamic damping coefficients, the example presented in this section is taken as a vehicle for illustrating the general qualitative characteristics of the model rather than the specific numerical values. Once additional information from experimental or analytical studies becomes available, new results will be incorporated in the model. The ultimate test of the model is to compare the analytical predictions with laboratory or field observations.

A. Stationary Fluid

In a stationary fluid, C, $\bar{C}$, H and $\bar{H}$ in Eq. (18) are zero; thus, in-plane and out-of-plane motions are uncoupled and the motions in the two directions can be studied independently. Free vibration for this case was considered previously [16].

In a heat exchanger tube bank, in most cases, all tubes are identical. Coupled natural frequencies for this case can be obtained rather easily. Assume that all tubes have the mass per unit length m ($m_i = m$) and the frequency in vacuo ω_n ($\omega_{in} = \bar{\omega}_{in} = \omega_n$). The natural frequencies of the coupled modes are given by [22]

$$\Omega_n = \left(\frac{m}{m + M'\sigma_n}\right)^{1/2} \omega_n \quad , \tag{28}$$

where σ_n are the eigenvalues of the added mass coefficient matrix $[\alpha_{ij}]$ or $[\beta_{ij}]$ (see Eqs. 4). Equation (28) shows that the natural frequency of a coupled mode can be calculated based on a single tube provided that the eigenvalue of the added mass matrix is taken as the effective added mass.

The effects of spacing and detuning on coupled natural frequencies have been studied; the results are summarized as follows:

1. In many practical cases, the spacing between the tubes is uniform. However, if a tube is displaced, the natural frequencies of coupled modes will be shifted. For example, if the central tube in a row of five tubes is displaced, the coupled natural frequencies will be more widely spread; that is, in a frequency band, the lowest natural frequency will be lower and the highest natural frequency will be higher than those of uniform spacing.

2. In a group of tubes, if a tube has a different frequency in vacuo from others, the natural frequencies of coupled modes are reduced if the tube has a lower frequency and increased if it is higher.

B. Natural Frequencies of Coupled Modes as Functions of the Flow Velocity

The dynamic behavior of a tube bank subjected to a cross flow can be studied based on Eq. (23). The natural frequency of the coupled tube-fluid system is designated by Ω, then the eigenvalue λ obtained from Eq. (23) is equal to $i\Omega$. The dynamic behavior of the system is determined by Ω: 1) when Ω is real, the system performs undamped oscillations; 2) when Ω is complex having a positive imaginary part, the system is stable and performs damped oscillations; 3) when Ω is complex having a negative imaginary part, the system loses stability by flutter; and 4) when Ω is imaginary, the system loses stability by buckling.

Figure 3 shows the natural frequencies of the lowest four modes for two tubes subjected to cross flow, where the numbers in the figure indicate the magnitude of flow velocity in m/sec. At low flow velocities, all modes are damped. As the flow velocity increases, the imaginary part of Ω may increase or decrease while there is a small increase in $\mathrm{Re}(\Omega)$. As the flow velocity is increased to a certain value, $\mathrm{Im}(\Omega)$ becomes zero and the tubes become unstable by flutter. For example, mode 1 becomes flutter at $V = 5.3$ m/sec and mode 3 at $V = 5.5$ m/sec.

At $V = 0$, the motions associated with the natural modes of a tube bank are rectilinear. However, for $V \neq 0$, due to the coupling effect of the fluidelastic forces, tube motions associated with the natural modes become orbital; these orbital movements associated with the two tubes are shown in Fig. 3.

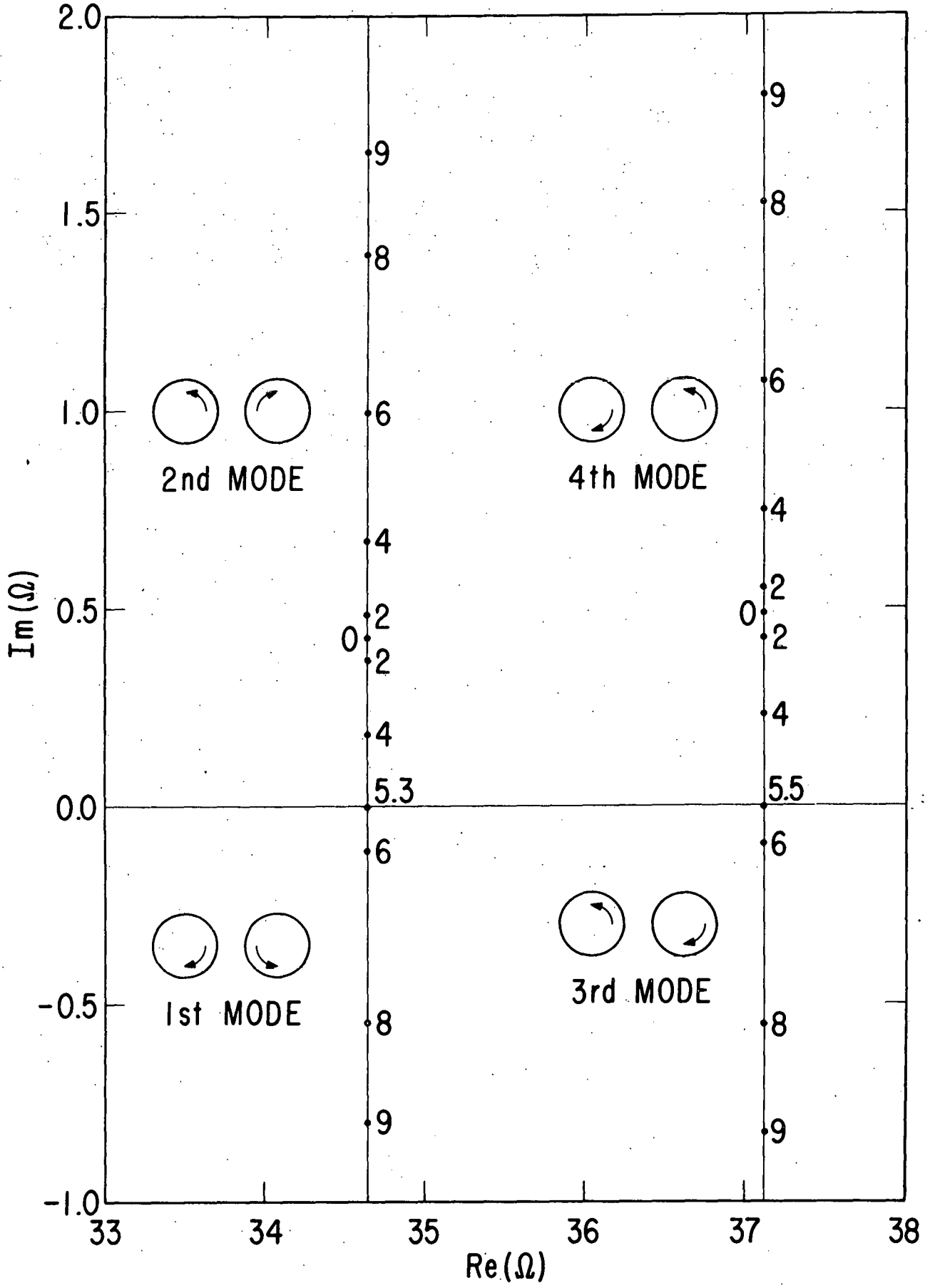

Fig. 3. Complex frequencies of two tubes subjected to a cross-flow

C. Critical Flow Velocities and Instability Modes

The critical flow velocities depend on system parameters in a complicate way and can be calculated from Eq. (23). A closed form solution for two identical tubes is obtainable. Assume that the properties of the constituent tubes, both in in-plane and out-of-plane directions, are as follows: natural frequency ω_n, damping ratio ζ_n, and mass per unit length m. In this case, Eqs. (23) are reduced to

$$[\gamma_{ij}]\{\bar{x}_j\} = \{0\} \quad ,$$

where

$$\gamma_{11} = \gamma_{22} = \gamma_{33} = \gamma_{44} = (m + \alpha_{11}M')\lambda^2 + 2m\zeta_n\omega_n\lambda + m\omega_n^2 \quad , \tag{29}$$

$$\gamma_{12} = \gamma_{21} = -\gamma_{34} = -\gamma_{43} = M'\alpha_{12}\lambda^2 \quad ,$$

$$\gamma_{13} = \gamma_{24} = \gamma_{31} = \gamma_{42} = 0 \quad ,$$

$$\gamma_{14} = -\gamma_{23} = -\frac{\rho V^2}{2}\nu \quad ,$$

$$\gamma_{32} = -\gamma_{41} = -\frac{\rho V^2}{2}\nu' \quad .$$

Using Routh-Hurwitz stability criterion, one can show that the critical flow velocity is given by

$$\frac{V}{f_c d} = \kappa \left[\frac{m_c (2\pi\zeta_c)}{\rho d^2}\right]^{1/2} \quad ,$$

where

$$m_c = m + M' (\alpha_{11} \pm \alpha_{12}) \quad , \tag{30}$$

$$\Omega_c = 2\pi f_c = \left(\frac{m}{m_c}\right)^{1/2}\omega_n \quad ,$$

$$\zeta_c = \frac{m\omega_n}{m_c\Omega_c}\zeta_n \quad ,$$

$$\kappa = \frac{2\sqrt{2\pi}}{\sqrt[4]{\nu\nu'}} \quad .$$

Equation (30) is similar to the original stability criterion developed by Connors [7] and reconsidered by Blevins [8]. There are two differences:

1. The instability flow velocities given by Eq. (30) are based on the coupled modes; m_c, f_c, and ζ_c are the virtual mass, natural frequency, and damping ratio of the coupled modes. On the other hand, Connors' criterion is based on those of a single tube.

2. There are multiple instability modes given in Eq. (30). Once the critical flow velocity is calculated, the instability mode shape can be determined from (23) or (29). But the instability mode of Connors' instability criterion has to be assumed before the critical flow velocity can be determined, and there is only one instability flow velocity because only one instability mode was considered.

Connors' criterion is developed for tube rows subject to air flows. The fluid inertia coupling effect is small, and a single tube consideration is satisfactory provided that reasonably accurate instability modes are taken. However, in a liquid flow, particularly when the tube spacing is small, fluid inertia coupling will be significant, and the stability criterion should be based on coupled modes.

Table 1 shows the critical flow velocity V_{cr} (m/sec) and the associated frequency (Hz) at instability for tube rows consisting of 2 to 7 tubes. For two tubes there are two modes of instability; however, for tube rows having more tubes, there are many more modes of instability. In Table 1, only those critical flow velocities less than 15 m/sec are given. Several distinct characteristics are noted:

1. The oscillation frequencies for various instability modes are relatively close, and the lowest critical flow velocity is not necessarily associated with the lowest oscillation frequency. For example, the five-tube row loses stability at V_{cr} = 5.49 m/sec with f_{cr} = 35.35 Hz, but the

TABLE 1

CRITICAL FLOW VELOCITY V_{cr} AND THE ASSOCIATED FREQUENCY f_{cr}

2 Tubes		3 Tubes		4 Tubes		5 Tubes		6 Tubes		7 Tubes	
V_{cr}	f_{cr}	V_{cr}	f_{cr}	V_{cr}	f_{cr}	V_{cr}	f_{cr}	V_{cr}	f_{cr}	V_{cr}	f_{cr}
5.32	34.64	8.22	36.60	5.26	35.27	5.49	35.35	5.32	35.35	4.58	35.51
5.50	37.12	8.47	36.15	5.33	36.52	5.64	34.42	5.46	36.22	5.00	36.25
				8.94	37.48	10.08	36.43	7.03	36.89	7.85	36.60
						11.62	35.69	11.69	37.55	8.67	35.46
										11.39	36.56

second critical flow velocity is 5.64 m/sec with the oscillation frequency of 34.42 Hz.

2. The lowest two critical flow velocities are relatively close to each other. Based on the linear theory, once the flow velocity reaches the critical value, large oscillations occur until the system is destroyed. In reality, other nonlinear effects, such as tubes impacting with one another, will limit the oscillation amplitudes. Since the second critical flow velocity is close to the first one, the instability modes observed in practical situations may change as the flow velocity is increased. This phenomena has been observed by Connors [7]. He observed that small changes in a tube row can cause a variety of modes without changing the critical flow velocity significantly.

3. The lowest critical flow velocities vary with the number of tubes in a tube array. In general, a tube row with more tubes is less stable. However, the critical flow velocity does not always decrease with tube number.

Figure 4 shows the lowest two instability modes for tube rows having 2, 3, 4, and 5 tubes and Fig. 5 shows the instability modes for a 7-tube row. The arrows on the orbital paths indicate the relative position of the tubes in the vibration orbits.

One instability mode frequently observed in experiments [7,17] is as follows: A tube vibrates predominantly in the streamwise direction, while its two neighboring tubes vibrate predominantly in the transverse direction with a phase shift of 180°, more precisely, this mode involved predominantly an up- and downstream movement of the central tube with transverse movement of the wing tubes such that the central tube moves downstream through a narrow gap and upstream through a wide gap. From Figs. 4 and 5, it is seen that many instability modes exhibit this behavior. For

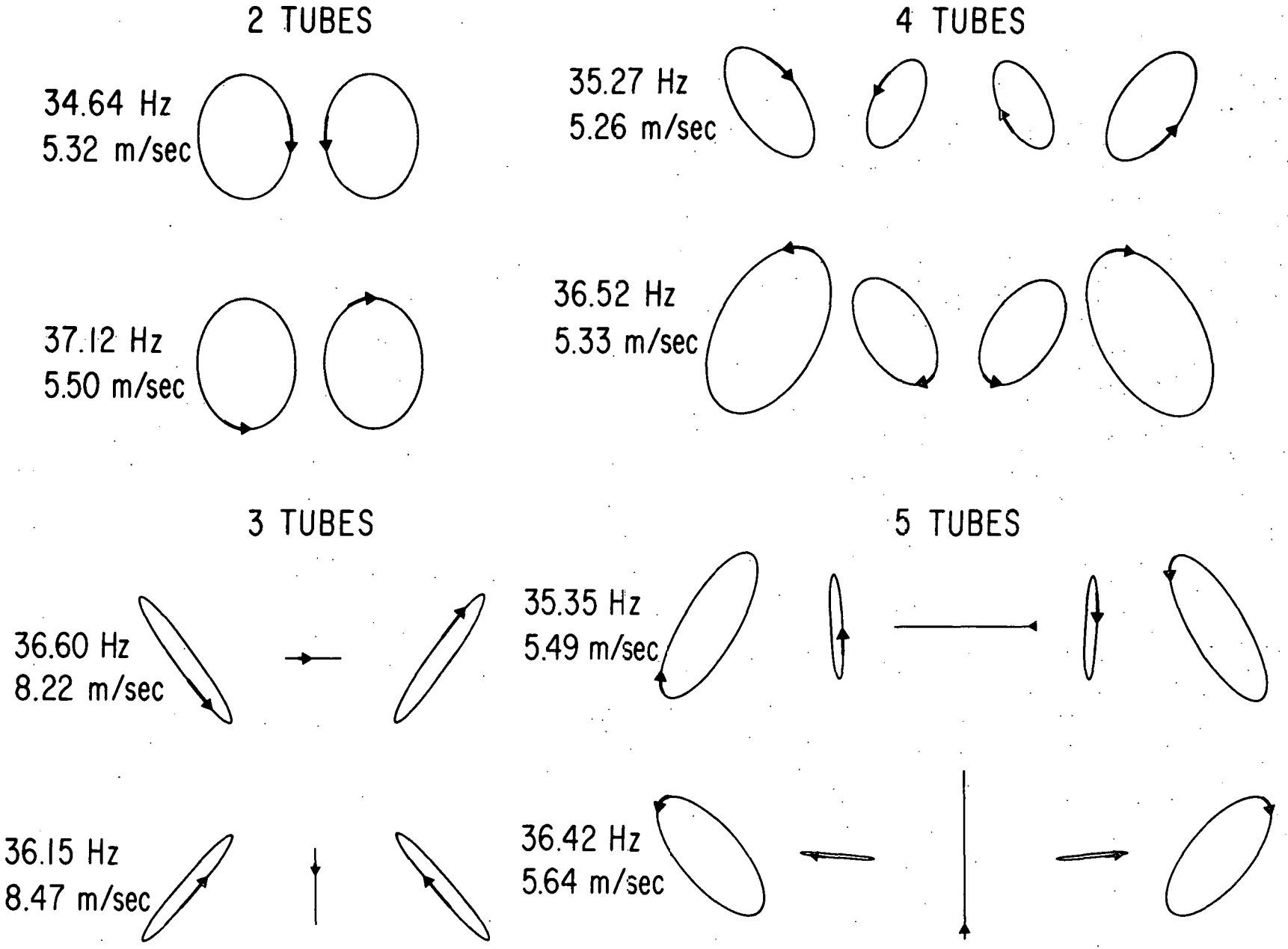

Fig. 4. Instability modes for 2, 3, 4 and 5 tubes

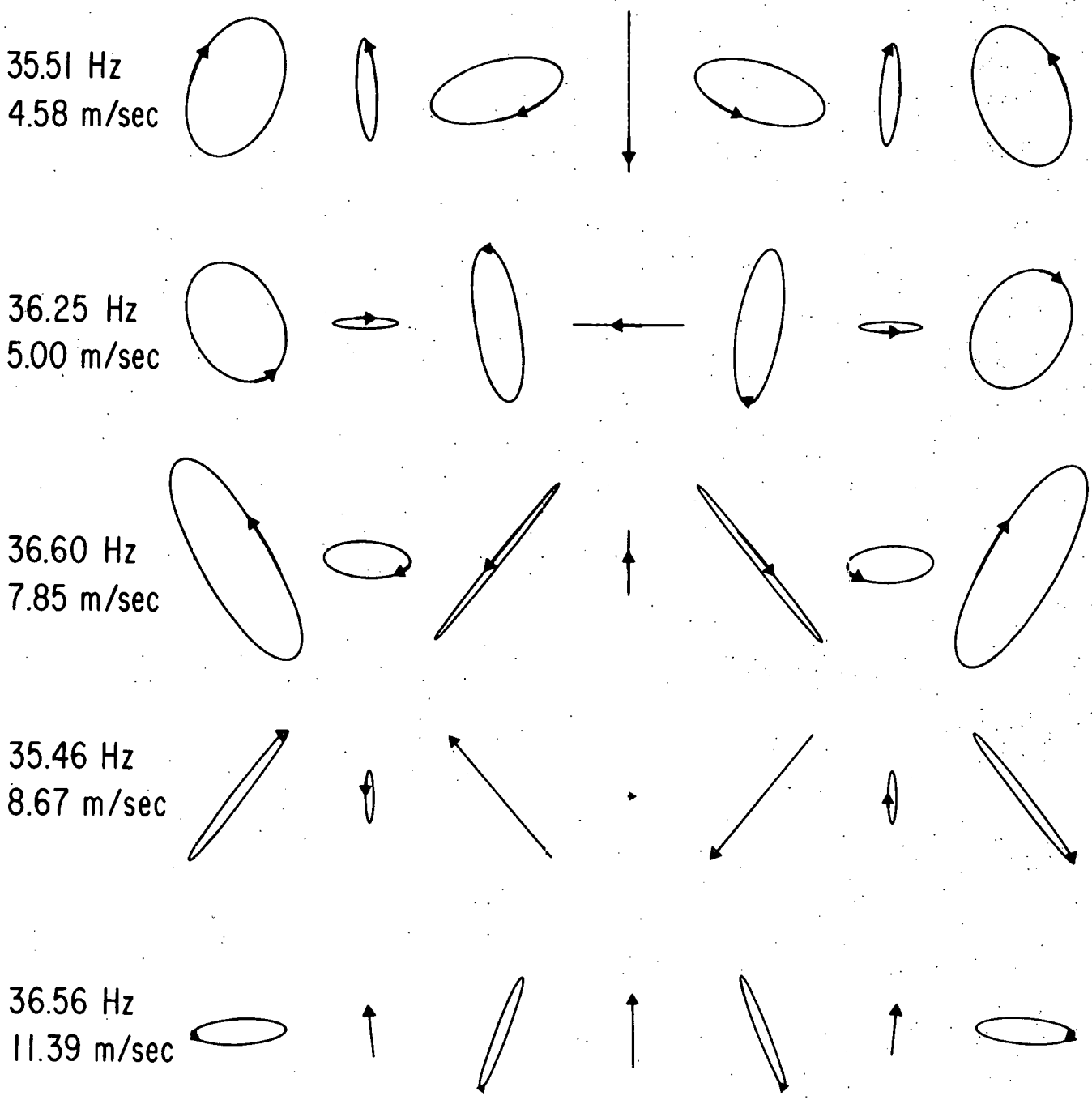

Fig. 5. Instability modes for 7 tubes

example, consider the second instability modes of 3 and 5 tubes and the first instability mode of 7 tubes. The orbital movements of the three adjacent tubes located in the middle of the row agree with Connors' experimental observations very well; indeed, the central tube moves downstream while the two wing tubes move out of phase to form a smaller gap.

D. Effects of System Parameters on Critical Flow Velocity

Numerical results for critical flow velocity presented so far are for tube rows consisting of identical tubes. In many practical situations, the tubes in an array may not be the same. The effects of system parameter variations are important in practical considerations. The effects detuning and damping have been investigated.

Figure 6 shows the lowest critical flow velocity for tube rows of 5 and 6 tubes as a function of the frequency ratio ω_A/ω_B. The natural frequency in vacuo for the tubes denoted by A is ω_A and by B is ω_B. The frequency ω_B is kept constant and ω_A is varied.

When the tubes are in tune, the critical flow velocity for cases 2, 3, and 4 are higher than those with a small detuning, while for case 1, the critical flow velocity at $\omega_A/\omega_B = 1$ corresponds to the minimum. As the tubes become more out-of-tune, the critical flow velocity increases and the lowest instability mode may also change. In reality, the tubes are probably not in tune; therefore, $\omega_A/\omega_B = 1$ is unlikely to occur in practical situations.

Based on Fig. 6, it can generally be concluded that detuning of the tubes in an array has beneficial effects from stability point of view. If fluidelastic instability is encountered in a design, using two different types of tubes arranged as case 1 in Fig. 6 is a way of solution. In case 1, the critical flow velocity increases rapidly with the detuning.

The results presented in Fig. 6 agree qualitatively with the experimental data obtained by Southworth and Zdravkovich [23]. It can also be used as a possible explanation of Baird's problem [24]. He reported that two "identical" boilers in the same plant exhibit entirely different vibration responses; sloppiness in tube installation will render one boiler non-responsive at design gas flow, while its accurately constructed mate

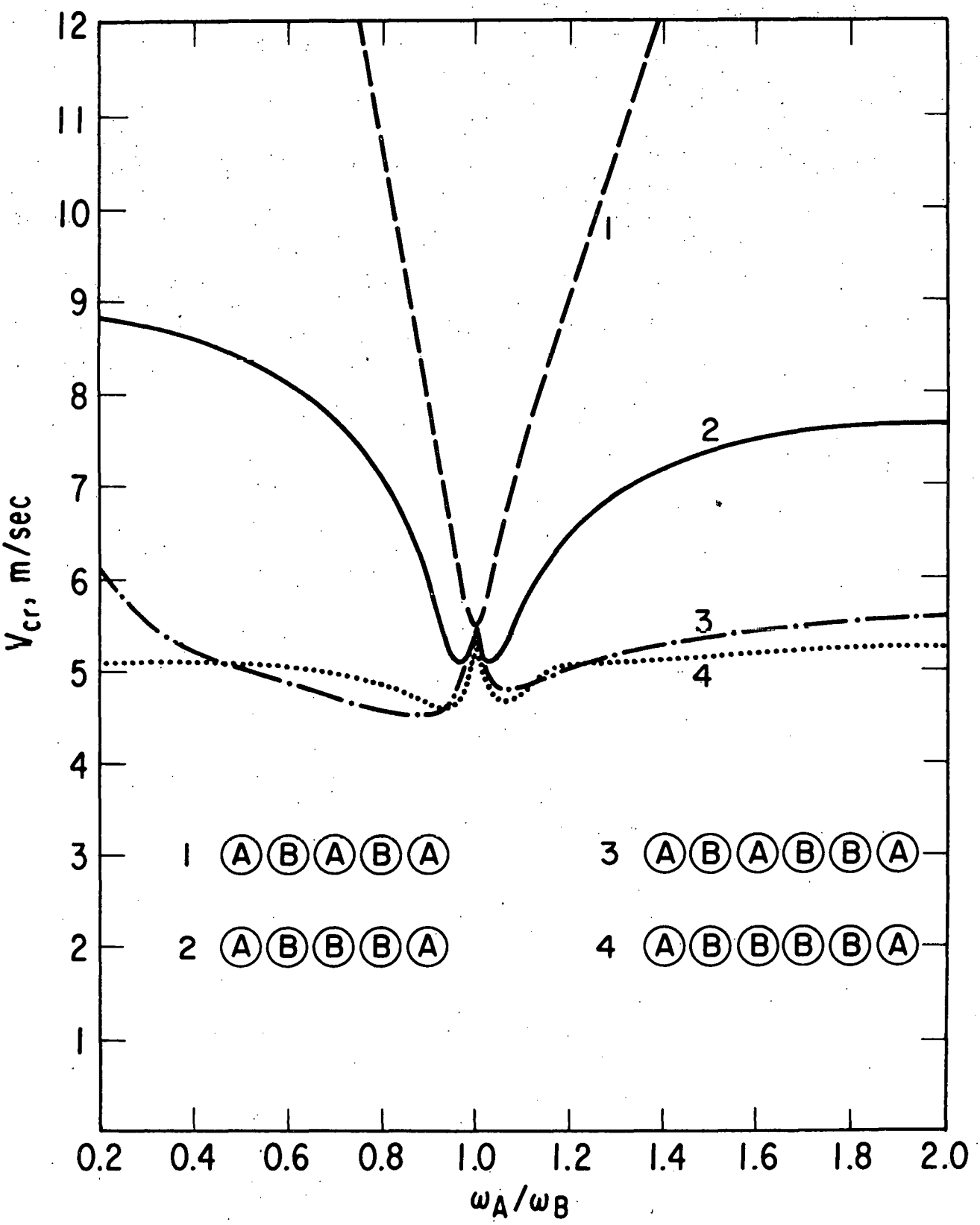

Fig. 6. Critical flow velocity as a function of frequency ratio of constituent tubes

pulsates with abandon. Based on Fig. 6, the natural frequencies of the sloppily constructed unit will be more out-of-tune; therefore, its critical flow velocity will be higher. At the design flow, the accurately constructed unit may be subject to instability, while the other is in the stable ranges of flow velocity.

Figure 7 shows the critical flow velocities as functions of viscous damping coefficient ratio, in which e_o is equal to 6.895 Pa-sec (0.001 lb-sec/in.^{2}). In general, the critical flow velocity increases as the values of the damping coefficient are increased. However, in some cases, the critical flow velocity may decrease with the increase of certain damping coefficients. As it can be seen from Fig. 7 for the case of three tubes, the critical flow velocity decreases when e_i/e_o is increased from 1 to about 2. The reason is as follows: When the damping coefficients are varied, the instability modes are also changed and increasing the values of certain damping coefficients may make certain modes more unstable; i.e., in those modes, the fluid energy is more easily fed into the tube system.

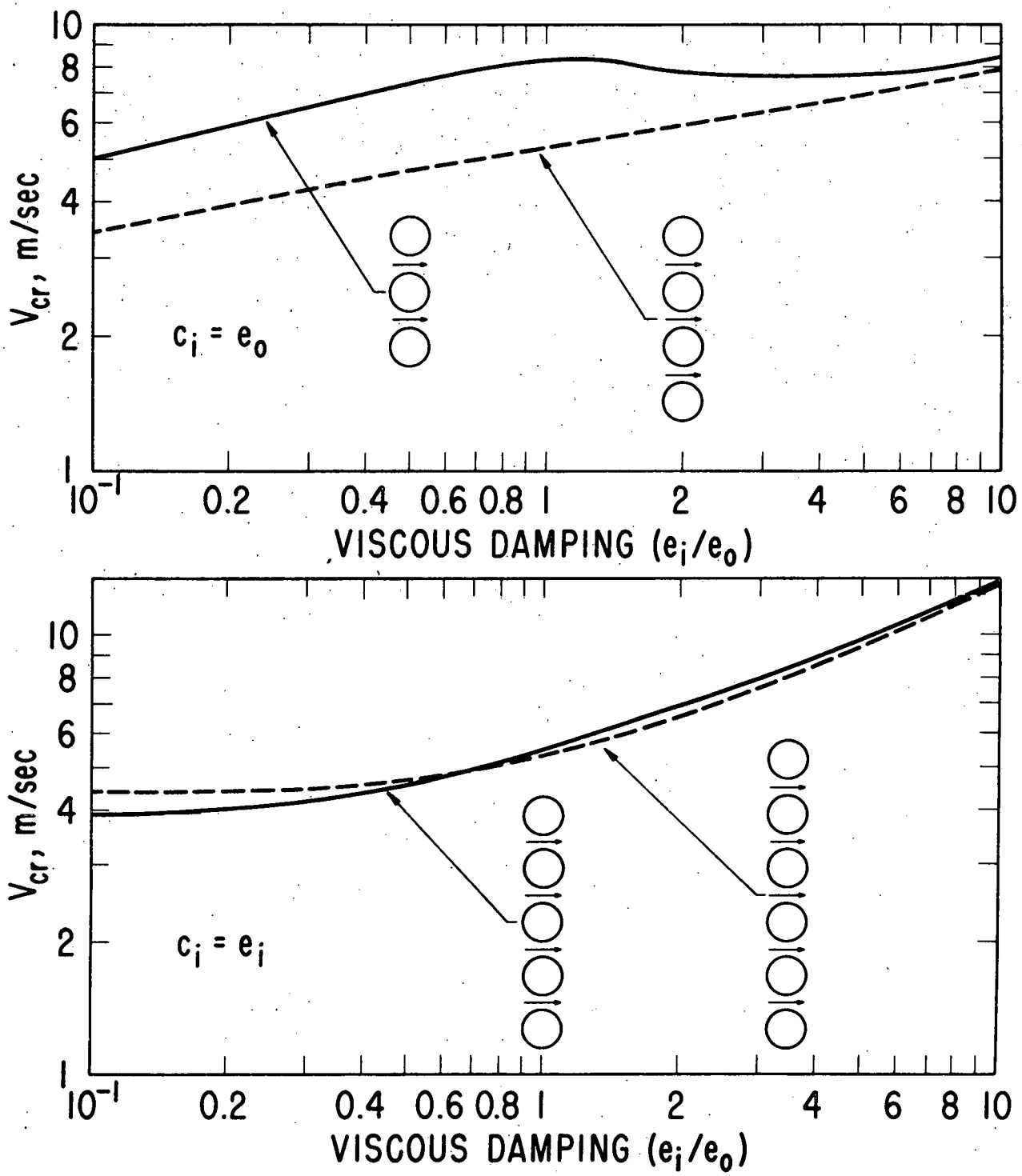

Fig. 7. Critical flow velocity as a function of viscous damping

E. Tube Responses as Functions of Flow Velocity

Two of the most important excitation mechanisms are vortex shedding and fluidelastic instability. Tube responses to those excitations are presented as functions of flow velocity to illustrate the interactions of those mechanisms.

Consider a row of five tubes, which are simply-supported at both ends. The tubes are subjected to vortices and fluidelastic forces. It is assumed that $c_i^{\ell} = 0.25$, $\psi_i^{\ell} = 0.0$, $\varepsilon_i = 0.0$, and $S = 0.2$. The steady-state responses of the tubes based on the coupled natural frequencies in the lowest frequency band are

$$u_i(z,t) = \bar{a}_i \sin(\omega_s t + \bar{\phi}_i) \sin\frac{\pi z}{\ell}$$
$$v_i(z,t) = \bar{b}_i \sin(\omega_s t + \bar{\psi}_i) \sin\frac{\pi z}{\ell} \qquad (31)$$

$u_i(z,t)$ and $v_i(z,t)$ are the displacement components of tube i in the lift and drag directions respectively. The values of $\bar{a}_1$, $\bar{b}_1$, $\bar{a}_3$, and $\bar{b}_3$ are given in Fig. 8.

The response characteristics can be divided into two regions: 1) vortex induced vibration for $V < 5.49$ m/sec; and 2) fluidelastic instability for $V > 5.49$ m/sec. At small flow velocities, the tubes respond predominantly in the lift direction. When the vortex shedding frequency synchronizes with the natural frequencies, tube 1 has a relatively large displacement component in the drag direction; this is due to the fluidelastic coupling effect. If there were no fluidelastic coupling, the tubes would have displacements only in the lift direction. Therefore, in the lower flow velocity region, the vortex shedding induces oscillations and the fluidelastic forces make the movement orbital. In the higher flow velocity ranges ($V > 5.49$ m/sec), the tubes are subjected to flutter type instability. The tube responses will become very large until other effects, such as impacting with other tubes, limit the motion or the tubes may be

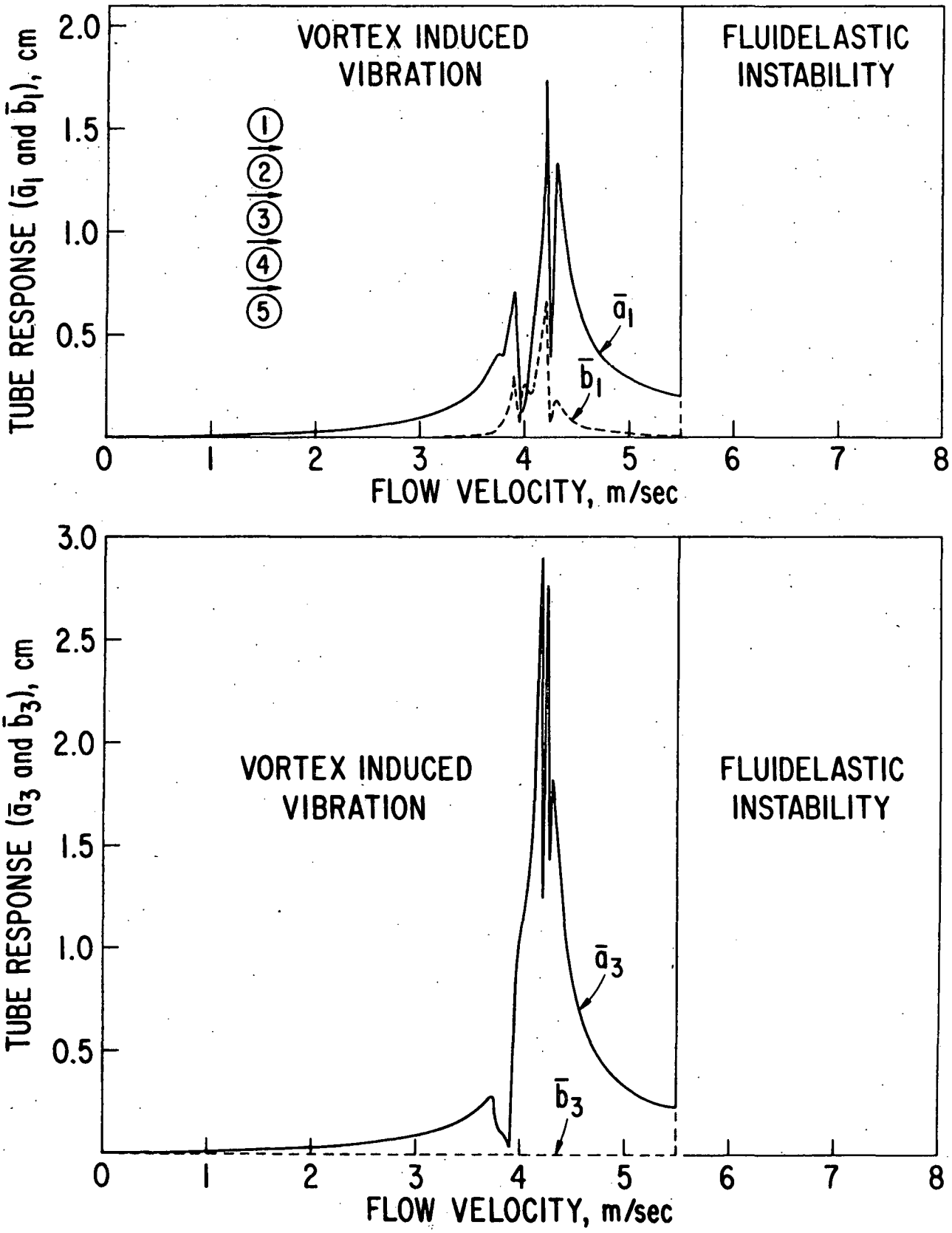

Fig. 8. Tube displacements as functions of flow velocity

damaged by large displacements. In the fluidelastic instability range, the motion is initiated by the vortex shedding or other flow noises, but it is the fluidelastic forces that produce large unstable orbital movement.

In this example, the vortex induced oscillations occur at the lower flow velocity. However, in other cases, the fluidelastic instability may occur at the lower flow velocity or both vortex induced vibration and fluidelastic instability may occur at the same flow velocity range. Since the model includes both mechanisms, it can be used to identify the dominant mechanism at a given flow velocity.

V. CONCLUSIONS

A mathematical model for cross-flow-induced vibrations of tube banks is presented. Once the force coefficients have been identified, this model can be used to find: (1) natural frequencies and natural modes of coupled tube-fluid system, and the effects of the fluid flow on vibrational characteristics; (2) critical flow velocities at which large tube oscillations occur and the instability modes; (3) responses of tube banks to lift force, drag force, and other flow noises; and (4) responses of tube banks to other types of excitations. The model is in agreement with the experimental results in stationary fluid [25]. In the flowing fluid, no experimental data are available for quantitative comparison. The experimental results published in the literature, such as those by Connors [7], Livesey and Dye [17], and Southworth and Zdravkovich [23], are in qualitative agreement with the analytical predictions.

Based on the results, several general conclusions can be made:

(a) Large tube oscillations may be associated with fluidelastic instability, vortex shedding, or other mechanisms. These mechanisms interact with one another; in each flow velocity range, there may be a dominant mechanism. Using a single mechanism to correlate all laboratory and field data is obviously not possible and is conceptually not sound.

(b) A tube bank subject to fluid flows will respond as an integrated system rather than as a collection of many individual tubes. This is attributed to fluid coupling effect. All the fluid coupling effects should be included in the model to obtain the proper description of orbital path of tube motion.

(c) The natural frequencies of coupled modes increase slightly with flow velocity, while the damping ratios of some modes decrease. When the flow velocity reaches a certain value, the damping of a certain

mode becomes zero and the tubes lose stability by flutter. Depending on system parameters, flutter flow velocity may be lower or higher than the "lock-in" flow velocity associated with vortex shedding.

(d) Detuning the tubes has a beneficial effect on flutter flow velocity. In particular, using two different tubes arranged in an alternate sequence drastically increases the flutter flow velocity.

(e) The flutter flow velocity increases with system damping. However, in certain cases, flutter flow velocity may decrease slightly, or remain nearly constant, with increasing damping because of change of instability modes.

(f) One of the most critical instability modes is associated with the mode that involves predominantly an up- and downstream movement of the central tube with transverse movement of the wing tubes such that the central tube moves downstream through a narrow gap and upstream through a wide gap.

(g) As the number of tubes in a tube bank increases, the flutter flow velocity, in general, decreases. Therefore, using a single-tube approximation may not be conservative.

(h) In the flow velocity range in which vortex shedding is dominant, although the excitation is in the lift direction, the tube will have a relatively large displacement in the flow direction because of fluidelastic coupling. On the other hand, in the flow velocity range in which fluidelastic instability is dominant, the motion may be initiated by other excitation mechanisms, but it is the fluidelastic coupling that produces large-amplitude oscillations.

The model will incorporate new theoretical and experimental results of the hydrodynamic forces as new information becomes available. A method of analysis to find the fluidelastic force and hydrodynamic damping using the potential flow theory is being developed [21]; the

results of this analysis and other experimental data will be incorporated in the model. The model also has been extended to the case of tube arrays which will be published in the future.

In conclusion, there is a great need for a useful mathematical model for cross-flow-induced vibrations of tube banks. The model presented in this report has demonstrated that it is capable of predicting the details of tube-fluid interactions including instabilities and responses to various types of excitations. With this model, improved design criteria can be established to eliminate detrimental flow-induced vibrations in tube banks.

ACKNOWLEDGMENT

This work was performed under the sponsorship of the Division of Reactor Development and Demonstration, U. S. Energy Research and Development Administration.

The author wishes to express his gratitude to Dr. M. W. Wambsganss for his comments on the report.

REFERENCES

1. H. K. Smith, "Vibrations in Nuclear Reactor Heat Exchangers - One Manufacturer's Viewpoint," Proc. Flow-Induced Vibration in Heat Exchangers, ASME, Winter Annual Meeting, New York, 1-7 (1970).
2. Y. N. Chen, "Flow-Induced Vibration and Noise in Tube-Bank Heat Exchanger due to von Karman Streets," J. Eng. Ind. 90(1), 134-146 (1968).
3. Y. N. Chen, "The Orbital Movement and the Damping of Fluidelastic Vibration of Tube Banks Due to Vortex Formation, Part 2 - Criterion for the Fluidelastic Orbital Vibration of Tube Arrays," ASME Paper No. 73-DET-146 (1973).
4. R. King and D. J. Johns, "Wake Interaction Experiments with Two Flexible Circular Cylinders in Flowing Water," Journal of Sound and Vibration 45 (2), 259-283 (1976).
5. O. M. Griffin and S. E. Ramberg, "Vortex Shedding from a Cylinder Vibrating in Line with an Incident Uniform Flow," J. Fluid Mech. 75, 257-271 (1976).
6. J. S. Fitz-Hugh, "Flow-Induced Vibration in Heat Exchangers," Proc. Vibration Problems in Industry, Paper No. 427, Keswick, England (1973).
7. H. J. Connors, Jr., "Fluidelastic Vibration of Tube Arrays Excited by Cross Flow," Sym. on Flow-Induced Vibration in Heat Exchangers, Winter Annual Meeting of ASME, New York, 42-56 (Dec. 1970).
8. R. D. Blevins, "Fluid Elastic Whirling of a Tube Row," ASME Paper No. 74-PVP-29 (1974).
9. D. J. Gorman and S. Mirza, "Experimental Development of Design Criterion to Limit Liquid Flow Induced Vibration in Nuclear Reactor Steam Generators," Presented at the 3rd SMiRT Conference, Paper No. F7/6 (1975).
10. H. Halle, B. L. Boers, and M. W. Wambsganss, "Fluidelastic Tube Vibration in a Heat Exchanger Designed for Sodium-to-Air Operation," J. of Eng. for Power, Trans. ASME 97, 561-568 (1975).

11. J. B. Erskine and W. Waddington, "A Review of Some Tube Vibration Failures in Shell and Tube Heat Exchangers and Failure Prediction Methods," Proc. Vibration Problems in Industry, Paper No. 421, Keswick, England (1973).

12. P. R. Owen, "Buffeting Excitation of Boiler Tube Vibration," J. Mech. Eng. Sci. 7(4), 431-439 (1965).

13. W. M. Walker and G. F. S. Reising, "Flow-induced Vibrations in Cross-flow Heat Exchangers," Chemical and Process Eng. 49(11), 93-103 (1968).

14. B. J. Grotz and F. R. Arnold, "Flow-Induced Vibrations in Heat Exchangers," Tech. Report No. 31, Dept. of Mech. Eng. Stanford Univ. (1956).

15. M. Funakawa and R. Umakoshi, "The Acoustic Resonance in a Tube Bank," Bulletin of the JSME 13(57), 348-355 (1970).

16. S. S. Chen, "Vibrations of a Row of Circular Cylinders in a Liquid," J. Eng. for Industry, Trans. ASME 97, 1212-1218 (1975).

17. J. L. Livesey and R. C. F. Dye, "Vortex Excited Vibration of a Heat Exchanger Tube Row," J. Mech. Eng. Science 4, 349-352 (1962).

18. A. R. J. Borges, "Vortex Shedding Frequencies of the Flow Through Two-Row Banks of Tubes," J. Mech. Eng. Science 11, 498-502 (1969).

19. R. C. F. Dye, "Vortex-Excited Vibration of a Heat Exchanger Tube Row in Cross-Flow," Proc. Vibration Problems in Industry, Keswick, England, 1973, Paper No. 417.

20. S. F. Hoerner, Fluid-Dynamic Drag, Published by the Author, 1965.

21. S. S. Chen, "Hydrodynamic Forces on a Group of Tubes Subjected to Cross-flows," To be published.

22. S. S. Chen, "Vibration of Nuclear Fuel Bundles," Nucl. Eng. Design 35, 399-422 (1975).

23. P. J. Southworth and M. M. Zdravkovich, "Cross-Flow-Induced Vibrations of Finite Tube Banks in In-Line Arrangements," J. Mech. Eng. Science 17 (4), 190-198 (1975).

24. R. C. Baird, Discussion on the paper "Flow-Induced Noise in Heat Exchangers," by A. A. Putnam, J. Eng. for Power, Trans. ASME 79, 417-422 (1959).

25. S. S. Chen and J. A. Jendrzejczyk, "Coupled Vibration of Two Parallel Tubes in a Liquid," presented at 1976 SESA Spring Meeting, Silver Springs, Maryland, May 9-14, 1976.